Biosensors and Bioelectronics 77 (2016) 277–283

Contents lists available at ScienceDirect

Biosensors and Bioelectronics

journal homepage: www.elsevier.com/locate/bios

Label-free DNA Y junction for bisphenol A monitoring using exonuclease III-based signal protection strategy

Junhua Chen, Shungui Zhou *

Guangdong Key Laboratory of Agricultural Environment Pollution Integrated Control, Guangdong Institute of Eco-Environmental and Soil Sciences, Guangzhou 510650, China

ARTICLE INFO

Article history:
Received 23 July 2015
Received in revised form
17 September 2015
Accepted 18 September 2015
Available online 25 September 2015

Keywords:
DNA Y junction
Exonuclease III
Label-free
Bisphenol A
Signal amplification

ABSTRACT

A label-free DNA Y junction sensing platform for the amplified detection of bisphenol A (BPA) has been constructed by the ingenious combination of toehold-mediated strand displacement and exonuclease III (Exo III)-based signal protection strategy. Three hairpin probes were utilized as the building blocks to fabricate the DNA Y junction with cascaded signal amplification *via* a series of toehold-mediated strand displacement reactions. Exo III was employed as a protecting agent for the first time to keep the Y-shaped molecular architecture intact, thereby greatly enhancing the fluorescence intensity of DNA intercalator SYBR Green I. The resulting biosensor exhibits ultrasensitivity towards BPA at low concentration (5 fM) without any labeling, modification, immobilization, or washing procedure. Our proposed sensing system also displays remarkable specificity to BPA against other possible interference molecules. Moreover, this DNA junction biosensor is robust and can be applied to the reliable monitoring of spiked BPA in environmental water samples with good recovery and accuracy. With the successful demonstration for BPA detection, the label-free DNA Y junction can be readily expanded to monitor other analytes in a simple, cost-effective, and ultrasensitive way by substituting the target-specific aptamer sequence.

1. Introduction

Bisphenol A (BPA) is an important monomer in the synthesis of polycarbonate (PC) and epoxy resins which are widely used for inner coating of feeding bottles, beverage containers, water supply pipes, and drug delivery carriers (Ragavan et al., 2013a). Tremendous amount of BPA can migrate into environment and food *via* wastewater discharge during the manufacturing process or by leaching from the packaging materials at high temperature (Geens et al., 2012). As an environmental endocrine disrupting chemical (EDC) with potential estrogenic activity, BPA can cause adverse health effects even at low concentrations (10^{-10} to 10^{-8} M) (Sheng and Zhu, 2011; Vandenberg et al., 2009). In addition, various types of cancers, cardiovascular disease, and diabetes are closely related to the intake of BPA (Tharp et al., 2012). Thus, routine detection of trace amounts of BPA with high sensitivity and selectivity is of critical importance for assuring food safety and human health.

Conventional techniques used in the quantification of BPA are mainly focused on instrument-based methods, such as high performance liquid chromatography (HPLC), liquid chromatography coupled with mass spectrometry (LC–MS), and gas chromatography coupled with mass spectrometry (GC–MS) (Ballesteros-Gomez et al., 2009). Although they offer high sensitivity and accuracy, those analytical techniques require expensive and sophisticated instrumentation, skilled operators, and time-consuming sample pre-treatment steps, which restrict their wide applications in routine measurements. To overcome these drawbacks, several groups have designed some elegant sensing strategies for colorimetric (Mei et al., 2013a; Ragavan et al., 2013b), electrochemical (Lee et al., 2011, 2014), and optical (Kuang et al., 2014; Marks et al., 2014; Zhu et al., 2015) detection of BPA by employing aptamers as the molecular recognition elements. Despite significant contributions have been made to BPA monitoring, most of these biosensors require specific labeling and immobilization procedures or extra separation and washing steps, resulting in not only a high cost of operation but also potentially complex processes. Thus, it is urgently needed to develop a label-free sensing system for BPA detection with high sensitivity, cost-effectiveness, and simplified operation.

Toehold-mediated DNA strand displacement reaction is a controllable nonenzymatic process in which one strand of DNA in a double-stranded complex is displaced by another DNA strand with the help of a short overhanging single-stranded domain (called a toehold) (Deng et al., 2014; Yin et al., 2008). Owing to its predictable thermodynamics and kinetics, this concept has been

* Corresponding author. Fax: +86 20 8702 5872.
E-mail address: sgzhou@soil.gd.cn (S. Zhou).

http://dx.doi.org/10.1016/j.bios.2015.09.042
0956-5663/

successfully exploited to construct DNA nanostructures (Hariadi et al., 2015; Huang et al., 2014; Sadowski et al., 2014), molecular logic circuits (Chen et al., 2015b; Fan et al., 2015; He et al., 2014; Li et al., 2013; You et al., 2015), catalytic amplifiers (Chen et al., 2013c; Qing et al., 2014), and even neural networks (Qian and Winfree, 2011; Qian et al., 2011). Remarkably, the toehold principle also exhibits some intriguing characteristics, such as continuous signal turnover capability, inherent modularity, and easy to scale up (Zhang and Seelig, 2011; Wang et al., 2014a). These unique attributes can provide an interesting magnified sensing approach for the detection of targets with much higher sensitivity (Chen et al., 2013a,b, 2014, 2015a; Jiang et al., 2015; Song et al., 2014). However, these reported biosensing techniques usually require fluorescent labeling or base modification to provide signal output (Huang et al., 2013; Jiang et al., 2014; Lei et al., 2014; Paliwoda et al., 2014). This in turn imposes strict limitation on the application of these techniques for bioassays. Hence, using toehold-mediated strand displacement to fabricate an ultrasensitive sensing platform without any label or modification remains a compelling goal.

Exonuclease III (Exo III) is a sequence-independent enzyme that does not require a specific recognition site and can catalyze the stepwise removal of mononucleotides from 3-hydroxyl terminus of duplex DNA in the case of substrate with a blunt or recessed 3′ terminus. Its activity on single-stranded DNA (ssDNA) or double-stranded DNA (dsDNA) with a protruding 3′ end is limited. With this property, Exo III-assisted target recycle strategies were widely reported to construct amplified detectors with enhanced signals (Freeman et al., 2011; Liu et al., 2012, 2014; Tao et al., 2015; Wu et al., 2014; Wang et al., 2014b; Zhang et al., 2013, 2014). However, there is no trial using Exo III as a protecting agent in biosensor design. Herein, for the first time, we developed a label-free DNA Y junction sensing platform for BPA detection with high sensitivity and selectivity by coupling toehold-mediated strand displacement with Exo III-based signal protection strategy. With the merits of cost-effectiveness, simplicity, versatility, and ultrasensitivity, the DNA Y junction sensing system will be a promising candidate for BPA detection in environmental monitoring, food control, and clinical diagnostics.

2. Experimental

2.1. Chemicals and materials

Bisphenol A (BPA), methanol, and tris-(hydroxymethyl)aminomethane (Tris) were purchased from Sigma-Aldrich (St. Louis, MO). SYBR Green I was purchased from Life Technologies (Grand Island, NY). Exonuclease III (Exo III) (1×10^5 U/mL) was purchased from New England Biolabs (Ipswich, MA). BPA was dissolved with methanol as the stock solution and diluted using the buffer solution for analysis. Other reagents and chemicals were of analytical grade and used without further purification. All solutions were prepared with ultrapure water (18.2 MΩ/cm) from a Millipore Milli-Q water purification system (Billerica, MA).

All oligonucleotides purified by HPLC were synthesized by Shanghai Sangon Biotechnology Co., Ltd. (Shanghai, China) and their sequences were listed in Table S1 (Supporting Information).

2.2. Construction of the DNA Y junction

The DNA solution was heated at 90 °C for 10 min and gradually cooled to room temperature at a constant rate over the course of 3 h to dissociate any intermolecular interaction. 100 nM DNA1 was initially incubated with 400 nM DNA2 in the reaction buffer (20 mM Tris–HCl, 100 mM NaCl, 25 mM KCl, 10 mM $MgCl_2$, pH=8.0) at room temperature for 30 min to form the DNA1–DNA2 duplex. BPA was then added into the above DNA1–DNA2 mixture and incubated at room temperature for 40 min to displace DNA2 and expose the toehold segment in DNA1. Subsequently, three hairpin DNA probes (hairpins A, B, and C, each was 2 μM) were added, and the mixture was incubated for 90 min at room temperature to generate the DNA Y junction structure (the A·B·C product). Finally, 35 units Exo III was added to the resulting solution, and the mixture was incubated for 30 min at room temperature.

2.3. Fluorescence detection

450 μL of the final sample solution was mixed with 50 μL of 10 × SYBR Green I solution. After incubation at room temperature for 5 min, the fluorescence spectra of the sensing system were recorded by a fluorescence spectrometer (Perkin-Elmer LS-55). The scanning wavelength ranged from 505 to 580 nm (λ_{ex}=495 nm, λ_{em}= 525 nm).

2.4. Procedure of the agarose gel electrophoresis

The 2% agarose gels contained 1 μL of ethidium bromide per 30 mL of gel volume were prepared using TBE buffer (1 ×). A volume of 8 μL of different DNA samples mixed with loading buffer (1 ×) was loaded into the lanes. Gel electrophoresis was performed at a constant potential of 100 V for 40 min and visualized under UV light by the gel image system.

2.5. Investigating the specificity of the sensor

To determine the specificity and selectivity of the developed method, several EDCs and a few other chemicals such as ethoxylated bisphenol A (BPE), bisphenol B (BPB), bisphenol C (BPC), bisphenol F (BPF), 4,4′-biphenol (4 BP), diethylstilbestrol (DES), 17β-estradiol (E2), estriol, and atrazine were tested at a concentration of 500 nM according to the procedures described above.

2.6. Analysis of actual water samples

The reliability of the sensor in practical applications was measured by determining the recovery rate in real water samples. Tap water samples were obtained from our laboratory. Lake water samples were collected from Jinkeng Reservoir (Guangzhou, China). River water samples were taken from the Pearl River (Guangzhou, China). Prior to analysis, all of the samples were filtered through a 0.22 μm membrane to remove the insoluble impurities. Aliquots of the water samples were spiked with different concentrations of BPA and diluted 5 times with the reaction buffer. Five duplicate measurements were performed for all samples. All analytical procedures were identical to those mentioned above.

3. Results and discussion

3.1. Design strategy for BPA detection

The design strategy for amplified detection of BPA on the basis of DNA Y junction and Exo III is schematically demonstrated in Scheme 1. DNA is represented as directional lines, with the squares denoting the 5′ termini and the arrows denoting the 3′ termini. The anti-BPA aptamer (Jo et al., 2011) was extended at the 5′-end to form a signal transducer strand (DNA1) where domain 1* is inhibited by hybridization with a complementary strand (DNA2). DNA2 should contain an appropriate number of bases so that it anneals to the aptamer with sufficient strength to offer low

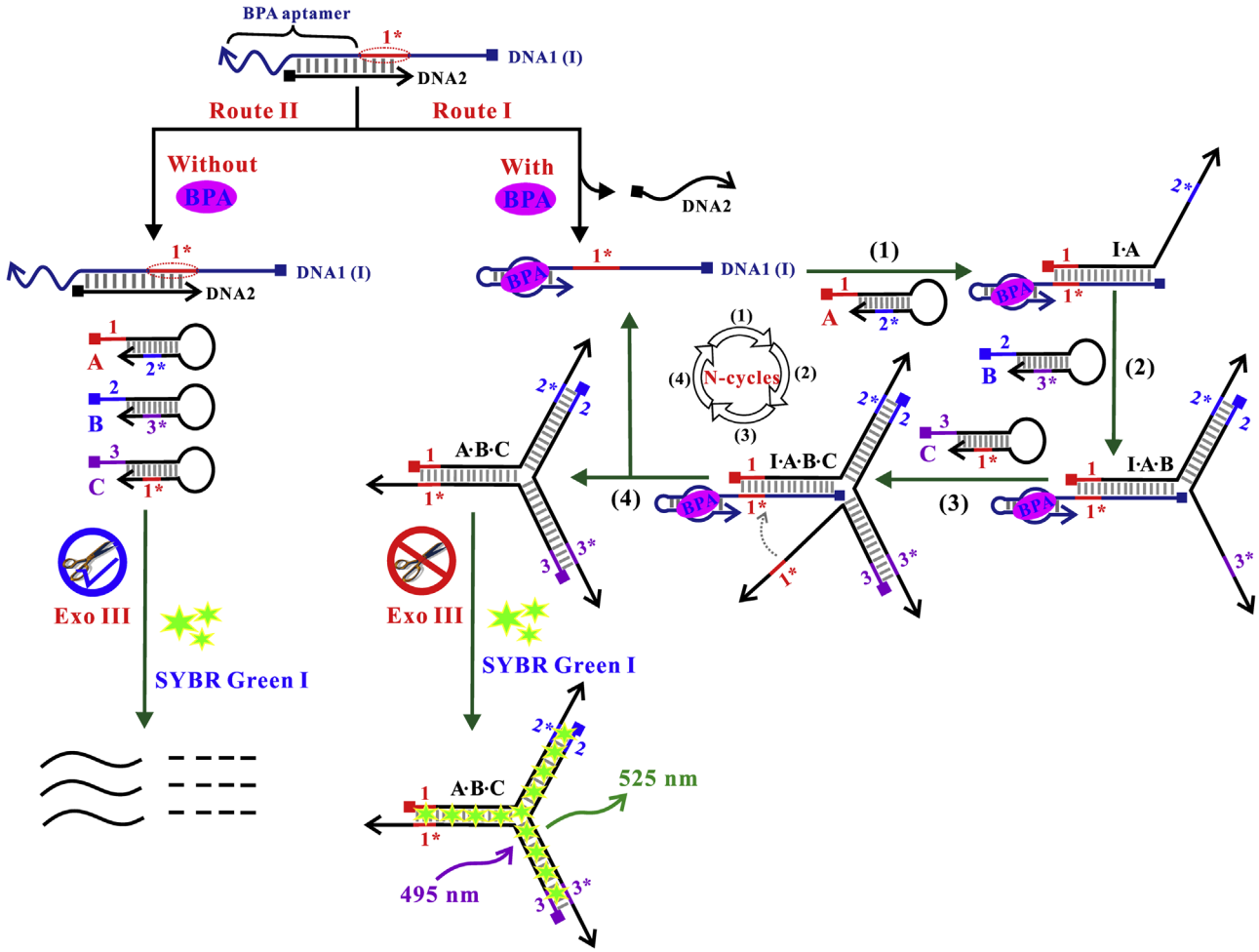

Scheme 1. Schematic representation of the design strategy for amplified detection of BPA on the basis of DNA Y junction and Exo III. The catalytic assembly is realized through a series of toehold-mediated strand displacement reactions (1, 2, 3, and 4) using three hairpins (A, B, and C) as the building blocks. Squares and arrows drawn on DNA strands represent 5′ termini and 3′ termini, respectively. Toeholds and toehold binding regions are named by numbers and complementarity is denoted by asterisks.

background fluorescence intensity in the absence of target. On the other hand, DNA2 should fast release from the aptamer when the target is present, which makes BPA easy to trigger the self-assembly of the hairpins. In the absence of BPA, domain 1* of DNA1 is occluded. When the ligand (in this case, BPA) binds to and stabilizes the aptamer strand (Scheme 1, route I), the partial duplex between DNA1 and DNA2 is destabilized and the single-stranded toehold (domain 1* of DNA1) is available to activate the subsequent strand displacement reaction. Three hairpin structures with protruding 5′ ends and recessed 3′ ends were selected as the building blocks (hairpins A, B, and C) to construct the signal amplification platform (Y junction architecture). The exposed domain 1* of the initiator DNA1 strand (I) first nucleates at the segment 1 of hairpin A and initiates a branch migration (toehold-mediated DNA strand displacement reaction) that opens hairpin A, leading to the formation of an I·A intermediate where the domain 2* of hairpin A is open (Scheme 1, reaction 1). Then, domain 2 of hairpin B can hybridize to the newly opened toehold 2* of hairpin A, again initiating a branch migration to open hairpin B and form an I·A·B hybrid where the segment 3* of hairpin B is no longer occluded (Scheme 1, reaction 2). Analogously, domain 3 of hairpin C can then bind to the newly accessible toehold 3* of hairpin B, triggering a strand displacement that opens hairpin C and generates an I·A·B·C complex (Scheme 1, reaction 3). The last step of the catalytic circle is the spontaneous dissociation of strand I from the A·B·C complex. During this process, the released I can be recycled to activate the self-assembly of additional hairpins (Scheme 1, reaction 4). The formed A·B·C product (DNA Y junction) with protruding 3′ ends is resistant to Exo III digestion due to the fact that Exo III only cleaves dsDNA with a blunt or recessed 3′ terminus. The intact dsDNA Y junction is then stained with SYBR Green I, resulting in a significantly amplified fluorescence signal toward BPA detection. In the absence of BPA (Scheme 1, route II), the initiator I should be catalytically inactive. The three hairpins A, B, and C are kinetically impeded from forming the Y junction. In this case, all hairpins and the DNA1–DNA2 duplex with recessed 3′ ends will be hydrolyzed by Exo III in the direction from 3′ to 5′, thus leaving ssDNA and mononucleotides in the sensing system. As SYBR Green I stains ssDNA with much lower intensity than dsDNA (Lin et al., 2014), only weak fluorescence background signal can be detected.

3.2. Feasibility of the sensing strategy

Agarose gel electrophoresis was used to confirm the formation of the DNA Y junction structure (A·B·C product) based on toehold-mediated strand displacement reactions. The electrophoresis results are shown in Fig. S1 (Supporting information). To further verify the feasibility of our designed signal amplification strategy for BPA detection, fluorescence emission spectra of the solution at different conditions were tested. As shown in Fig. 1, the solution containing DNA1–DNA2 and hairpins A, B, and C exhibited very weak fluorescence emission (curve *a*) in the absence of BPA (the background signal of SYBR Green I), which indicated that, without

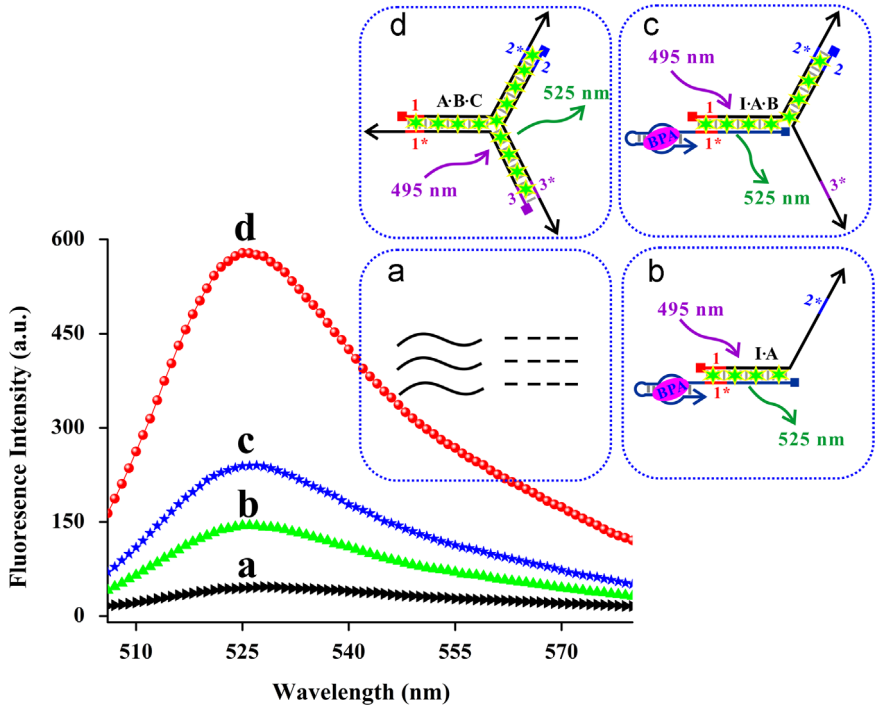

Fig. 1. Fluorescence spectra of the system under different conditions: (a) no BPA, DNA1–DNA2, hairpins A, B, and C, (b) 10 nM BPA, DNA1–DNA2, hairpin A, (c) 10 nM BPA, DNA1–DNA2, hairpins A and B, and (d) 10 nM BPA, DNA1–DNA2, hairpins A, B, and C. SYBR Green I: 1 × ; Exo III: 35 U. The experiments were performed at room temperature (~25 °C). The corresponding error bars in Fig. 1 represent the standard deviation of three independent measurements obtained under different conditions.

target introduction, the hairpins and DNA1–DNA2 duplex with recessed 3′ ends could be digested by Exo III. Upon the addition of BPA to the system containing DNA1–DNA2 and only hairpin A, the fluorescence intensity was obviously increased (curve *b*). That is because the formed I · A with protruding 3′ end is resistant to Exo III digestion, leaving dsDNA for SYBR Green I staining. Significantly, when both hairpins A and B were present in the mixture, further enhanced fluorescence was observed (curve *c*). Such increase was attributed to the formation of longer dsDNA in the I · A · B compound with protruding 3′ ends. Most importantly, a dramatic increase of the fluorescence signal was obtained (curve *d*) upon simultaneous addition of hairpins A, B, and C to the sensing system. This is most likely a consequence of the fact that a single BPA molecule can trigger recycling assembly of the three hairpins to generate A · B · C products, thereby resulting in the formation of numerous dsDNA to give an amplified fluorescence signal. The above results indicated that our proposed dsDNA Y junction sensing system can be utilized for amplified detection of target BPA.

3.3. Optimization of assay conditions

The assay conditions (*e.g.*, the molar ratio of DNA1 to DNA2, the reaction temperature of the sensing system, the reaction time of the toehold-mediated strand displacement reaction, and the concentration of the hairpin DNA) that affect the sensitivity and reproducibility of the Y junction sensing system were optimized. The optimizations were performed by varying one experimental condition and keeping constant conditions for other parameters. Using a fixed concentration (100 nM) of DNA1, the effect of molar ratio of DNA1 to DNA2 on the response of the biosensor was first evaluated by detecting 10 nM BPA. As shown in Fig. S2 (Supporting information), the signal-to-noise (*S*/*N*) ratio increased with the increment of the molar ratio of DNA1 to DNA2 from 1:1 to 1:4, further increasing the molar ratio caused a decrease of the *S*/*N* ratio. The reason for this result is that too much DNA2 would induce an insufficient displacement reaction between BPA and DNA1, thus resulting in a weak fluorescence signal. In contrast, deficient amount of DNA2 would generate unstable DNA1–DNA2 duplexes and cause a high background signal. Therefore, the molar ratio of DNA1 to DNA2 of 1:4 was used for BPA detection to achieve the best signal-to-noise level.

Another factor taken into account for parameter optimization is the reaction temperature, since it directly affects the binding kinetics among the hairpins and the activity of Exo III. The effect of the reaction temperature on the performance of the system was investigated by detecting 10 nM BPA at different temperature (4 °C, 25 °C, 37 °C, 40 °C, 42 °C and 45 °C). The blank sample (in the absence of BPA) at each temperature was tested at the same conditions. As shown in Fig. 2, the fluorescence intensity increased with the increase of the temperature in the range from 4 to 37 °C in the presence of 10 nM BPA and then decreased in the range from 37 to 45 °C (red histogram in Fig. 2). However, on the other hand, the conformation of the hairpin DNA would be destroyed as the increase of the reaction temperature, which increased the background signal (gray histogram in Fig. 2). Additionally, the exonuclease also cleaves some of the hairpin DNA under a relatively high temperature (Chen et al., 2014). In order to obtain the best *S*/*N* ratio (blue line in Fig. 2), an optimum reaction temperature of 25 °C was adopted in the following experiments. The *S*/*N* is defined as the specific signal-to-unspecific signal ratio. Because not just the level of the unspecific signal (0 nM measurement) but also its error is important for identifying the best assay conditions, (*S*–*N*)/std(*N*) is used to calculate the signal-to-noise ratio (std(*N*) is the standard deviation of three independent measurements for the unspecific signal in the absence of target). The corresponding error bars in Fig. 2 represent the standard deviation of three independent measurements obtained at each reaction temperature.

The performance of signal amplification and detection of BPA was strongly affected by the reaction time of the toehold-mediated strand displacement. To optimize the reaction time, we determined the fluorescence response at 25 °C. As demonstrated in Fig. 3, in the presence of target (10 nM, 100 pM, or 1 pM BPA), with

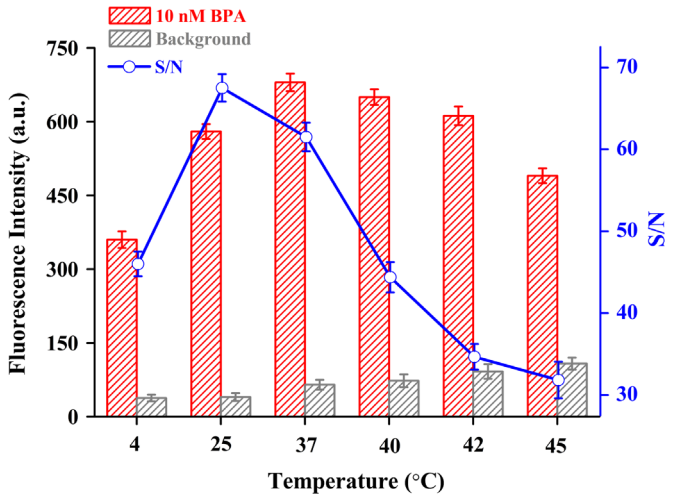

Fig. 2. Effect of the reaction temperature on the response of the sensing system. The histograms represent fluorescence intensity of the solution in the presence of 10 nM BPA (red) and in the absence of target (gray), respectively. The blue line represents the *S*/*N* ratio. (*S*–*N*)/std(*N*) is used to calculate the signal-to-noise ratio (std(*N*) is the standard deviation of three independent measurements for the unspecific signal in the absence of target). The corresponding error bars in Fig. 2 represent the standard deviation of three independent measurements obtained at each reaction temperature. (For interpretation of the references to color in this figure legend, the reader is referred to the web version of this article.)

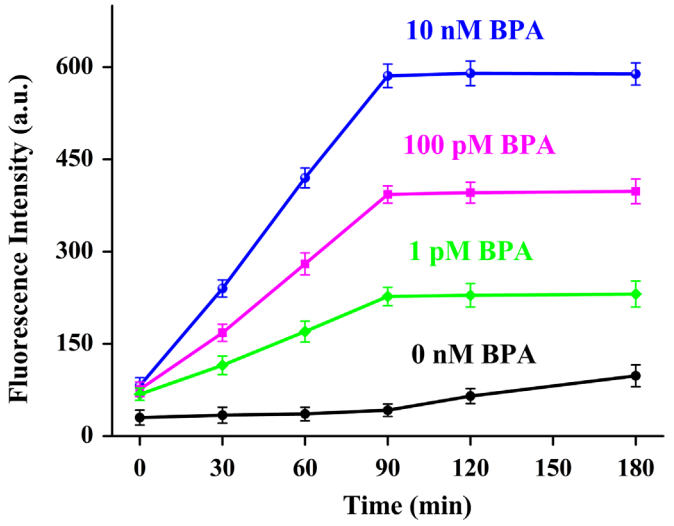

Fig. 3. Effect of the reaction time of toehold-mediated strand displacement on the response of the biosensor. Time course of fluorescence response recorded in the absence of BPA (black line) or in the presence of 10 nM, 100 pM and 1 pM BPA (blue, pink, and green lines). The experiments were performed at room temperature (~25 °C). The corresponding error bars in Fig. 3 represent the standard deviation of three independent measurements obtained at each reaction time. (For interpretation of the references to color in this figure legend, the reader is referred to the web version of this article.)

the reaction time increased gradually, the fluorescence intensity rose accordingly. Meanwhile, the fluorescence intensity started to plateau after 90 min (blue, pink, and green lines in Fig. 3). The enhanced signal within 90 min validated the feasibility of the amplification process, suggesting the continuous formation of the A · B · C products, while the plateau phenomenon indicated that almost all of the hairpins (A, B, and C) were depleted and converted into A · B · C products. However, in the control experiments without BPA, as the time prolonged, the background signal increased gradually (black line in Fig. 3). To achieve the best signal-to-background level and the maximal signal amplification efficiency, 90 min was employed as the optimum reaction time.

In this work, the detectable signal of the sensing system mainly derives from the formation of the A · B · C product, which indirectly relies on the concentration of the three hairpin DNA. As exhibited in Fig. S3 (Supporting information), increasing the hairpin concentration from 0.5 to 2 μM in the presence of 10 nM BPA was found to correspondingly increase the fluorescence intensity of the solution, and then the signal tended to level off when the hairpin DNA was higher than 2 μM (red histogram in Fig. S3). Unfortunately, the fluorescence response without target was also enhanced with the increase of the hairpin DNA concentration (gray histogram in Fig. S3). Although the high-concentration hairpin DNA is conducive to form the A · B · C product, it often suffers from high background signals. Hence, 2 μM hairpin DNA was found to be optimum here because it gave the maximum net signal (blue histogram in Fig. S3) for BPA detection.

3.4. Sensing performance for BPA detection

To evaluate the sensitivity and dynamic range of the proposed DNA Y junction sensing platform, different concentrations of BPA were examined under the optimal experimental conditions. As shown in Fig. 4A, a gradual increase of fluorescence intensity was observed by increasing the BPA concentrations in the range of 0–100 nM. Fig. 4B presented the relationship between the fluorescence intensities at 525 nm and the concentrations of BPA. The resulting calibration curve shows that the fluorescence intensity is linearly dependent on the logarithm of BPA concentration ranging from 10 fM to 10 nM with a correlation coefficient (R^2) of 0.98. The sensing system possesses a high sensitivity for BPA, with a limit of detection (LOD) of 5 fM. The detection limit is defined by $3S_0/S$ (Chen et al., 2009; Chen and Zeng, 2013; Hernandez and Escriche, 1984), where 3 is the factor at the 99% confidence level, S_0 is the standard deviation of the blank measurements ($n=15$), and S is the slope of the calibration curve (inset in Fig. 4B). The LOD of 5 fM of our constructed biosensor is at least three orders of magnitude better than the aptamer-based colorimetric biosensor for BPA without signal amplification (Mei et al., 2013a). Compared with previously reported BPA sensors based on immunoassay, the new DNA Y junction sensing platform developed here also possesses higher sensitivity (Long et al., 2014; Mei et al., 2013b). The excellent sensitivity mainly relied on the continuous turnover capability of the toehold-mediated strand displacement reaction to generate numerous dsDNA Y junctions even at low concentration of target BPA and the specific cleavage activity of Exo III, which can minimize the background signal. These results demonstrate that our constructed sensing platform can ensure simple, rapid, and ultrasensitive detection of BPA.

3.5. Selectivity and real sample analysis

The selectivity of the sensing system for BPA was evaluated by testing the fluorescence response of the assay to other control molecules, including ethoxylated bisphenol A (BPE), bisphenol B (BPB), bisphenol C (BPC), bisphenol F (BPF), 4,4′-biphenol (4 BP), diethylstilbestrol (DES), 17β-estradiol (E2), estriol, and atrazine, which may coexist in environment or have similar structure with BPA. As shown in Fig. 5, only BPA (10 nM) makes the fluorescence intensity increase obviously. The sensor hardly exhibits substantial responses to other control molecules (500 nM) and the fluorescence change is almost neglectable compared with the blank sample. Those data suggested that our developed amplification approach exhibited excellent selectivity for BPA detection. The high specificity is attributed to the specific binding capability of the aptamer to the target BPA. In other words, only the presence of BPA can associate with the aptamer segment and activate the toehold domain to initiate the toehold-mediated strand

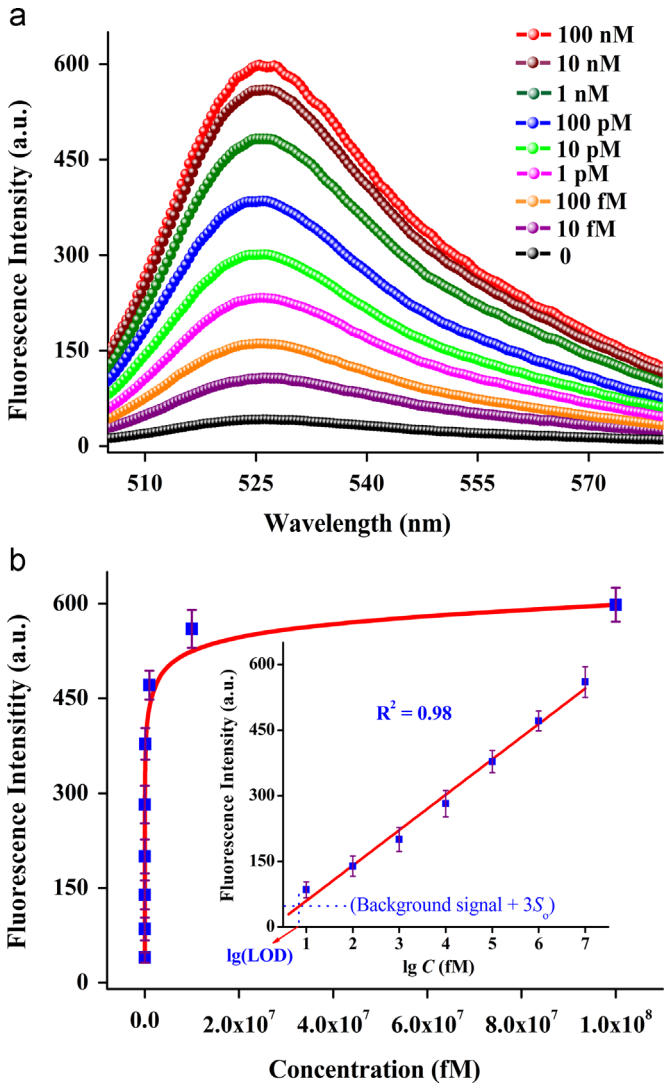

Fig. 4. (A) Fluorescence spectra upon addition of different concentrations of BPA. (B) Plots of the fluorescence intensity at 525 nm as a function of the BPA concentration. Inset: linear relationship between the fluorescence intensity and the logarithm of BPA concentration in the range from 10 fM to 10 nM. S_0 is the standard deviation of the blank measurements ($n=15$). The corresponding error bars in Fig. 4B represent the standard deviation of three independent measurements obtained at different concentrations of BPA.

displacement reaction to generate numerous dsDNA Y junction products for fluorescence readout.

With the excellent selectivity and sensitivity, our proposed method was further tested with several environmental water samples (tap water, lake water, and river water) to demonstrate its ability for practical applications. These samples spiked with three different concentrations of 0, 0.05, 10, 100, 1000 pM BPA were determined with five replicates. The recovery results of BPA in the three different matrixes were summarized in Table S2 (Supporting information). The recovery of all measured samples and the relative standard derivations (RSD) ranged from 90–118% and 1.7–5.7%, respectively, revealing that the possible interference from the different complex matrices of water samples on the sensor analysis was negligible. The above results demonstrate that our developed DNA Y junction sensing platform can be successfully applied to BPA detection in real environmental water samples.

4. Conclusions

In summary, we have successfully fabricated, for the first time,

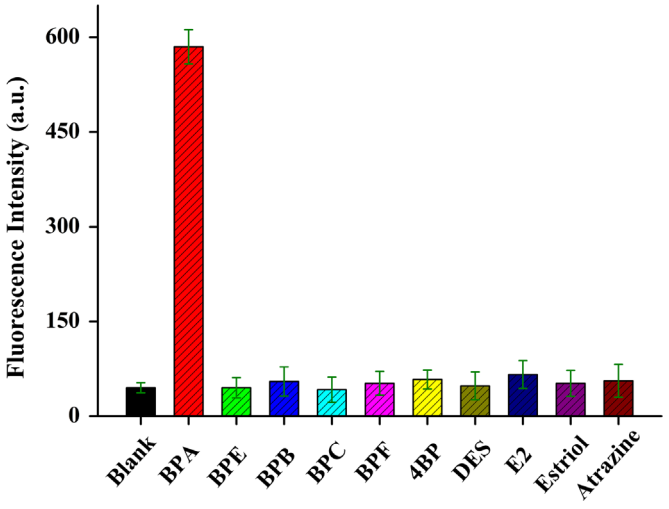

Fig. 5. Selectivity of the sensing system analyzing BPA over other control molecules. The concentration is 10 nM for BPA and 500 nM for other molecules. The corresponding error bars in Fig. 5 represent the standard deviation of three independent measurements obtained at different analytes.

a label-free biosensor for the amplified detection of BPA using a DNA Y junction for signal transduction. The Y junction sensing platform is formed on the basis of toehold-mediated strand displacement and Exo III-induced signal protection strategy. Due to the cascaded signal amplification efficiency of a series of toehold-mediated strand displacement reactions and the signal protection capacity of Exo III, the presence of trace amounts of BPA leads to the generation of numerous intact Y-shaped molecular architectures, which result in enhanced fluorescence intensity of the reaction solution for ultrasensitive detection of BPA down to 5 fM. Meanwhile, our approach afforded exquisite selectivity for BPA against other possible interference molecules. This sensor is robust and can be applied to the reliable monitoring of spiked BPA in environmental water samples with good recovery and accuracy. The construction strategy herein is simple in design and economic in operation without labeling and immobilization procedures or separation and washing steps, making this DNA Y junction sensing system particularly suitable for routine monitoring of BPA in environmental and biological samples. Importantly, this sensing platform is modular and versatile and can be easily extended to the analysis of other analytes by simply choosing other aptamers as the molecular recognition elements.

Acknowledgments

Financial support was provided by the National Natural Science Foundation of China (Grant nos. 21407029 and 41401261), the Natural Science Foundation of Guangdong Province (Grant no. 2014A030313705), the Science and Technology Program of Guangzhou (Grant no. 201508020010), the Key Projects in the National Science & Technology Pillar Program of China (Grant no. 2015BAD06B03), and the Pearl River S&T Nova Program of Guangzhou (Grant no. 201506010093).

Appendix A. Supporting material

Supplementary data associated with this article can be found in the online version at http://dx.doi.org/10.1016/j.bios.2015.09.042.

References

Ballesteros-Gomez, A., Rubio, S., Perez-Bendito, D., 2009. J. Chromatogr. A 1216, 449–469.
Chen, J., Wen, J., Yang, G., Zhou, S., 2015a. Chem. Commun. 51, 12373–12376.
Chen, J., Zeng, L., 2013. Biosens. Bioelectron. 42, 93–99.
Chen, J., Zhou, S., Wen, J., 2014. Anal. Chem. 86, 3108–3114.
Chen, J., Zhou, S., Wen, J., 2015b. Angew. Chem. Int. Ed. 54, 446–450.
Chen, J., Zhou, X., Zeng, L., 2013a. Chem. Commun. 49, 984–986.
Chen, S.X., Zhang, D.Y., Seelig, G., 2013b. Nat. Chem. 5, 782–789.
Chen, X., Briggs, N., McLain, J.R., Ellington, A.D., 2013c. Proc. Natl. Acad. Sci. USA 110, 5386–5391.
Chen, Z., Liu, G., Chen, M., Peng, Y., 2009. Anal. Biochem. 384, 337–342.
Deng, R., Tang, L., Tian, Q., Wang, Y., Lin, L., Li, J., 2014. Angew. Chem. Int. Ed. 53, 2389–2393.
Fan, D., Wang, K., Zhu, J., Xia, Y., Han, Y., Liu, Y., Wang, E., 2015. Chem. Sci. 6, 1973–1978.
Freeman, R., Liu, X., Willner, I., 2011. Nano Lett. 11, 4456–4461.
Geens, T., Aerts, D., Berthot, C., Bourguignon, J., Goeyens, L., Lecomte, P., Maghuin-Rogister, G., Pironnet, A., Pussemier, L., Scippo, M., Loco, J.V., Covaci, A., 2012. Food Chem. Toxicol. 50, 3725–3740.
Hariadi, R.F., Yurke, B., Winfree, E., 2015. Chem. Sci. 6, 2252–2267.
He, X., Li, Z., Chen, M., Ma, N., 2014. Angew. Chem. Int. Ed. 53, 14447–14450.
Hernandez, F.H., Escriche, J.M., 1984. Analyst 109, 1585–1588.
Huang, F., Xu, H., Tan, W., Liang, H., 2014. ACS Nano 8, 6849–6855.
Huang, F., You, M., Han, D., Xiong, X., Liang, H., Tan, W., 2013. J. Am. Chem. Soc. 135, 7967–7973.
Jiang, Y.S., Bhadra, S., Li, B., Ellington, A.D., 2014. Angew. Chem. Int. Ed. 53, 1845–1848.
Jiang, Y.S., Bhadra, S., Li, B., Wu, Y.R., Milligan, J.N., Ellington, A.D., 2015. Anal. Chem. 87, 3314–3320.
Jo, M., Ahn, J., Lee, J., Lee, S., Hong, S.W., Yoo, J., Kang, J., Dua, P., Lee, D., Hong, S., Kim, S., 2011. Oligonucleotides 21, 85–91.
Kuang, H., Yin, H., Liu, L., Xu, L., Ma, W., Xu, C., 2014. ACS Appl. Mater. Interfaces 6, 364–369.
Lee, J., Jo, M., Kim, T.H., Ahn, J., Lee, D., Kim, S., Hong, S., 2011. Lab Chip 11, 52–56.
Lee, J.S., Kim, S.G., Jun, J., Shin, D.H., Jang, J., 2014. Adv. Funct. Mater. 24, 6145–6153.
Lei, C., Huang, Y., Nie, Z., Hu, J., Li, L., Lu, G., Han, Y., Yao, S., 2014. Angew. Chem. Int. Ed. 53, 8358–8362.
Li, W., Yang, Y., Yan, H., Liu, Y., 2013. Nano Lett. 13, 2980–2988.
Lin, C., Cai, Z., Wang, Y., Zhu, Z., Yang, C.J., Chen, X., 2014. Anal. Chem. 86, 6758–6762.
Liu, S., Lin, Y., Wang, L., Liu, T., Cheng, C., Wei, W., Tang, B., 2014. Anal. Chem. 86, 4008–4015.
Liu, X., Aizen, R., Freeman, R., Yehezkeli, O., Willner, I., 2012. ACS Nano 6, 3553–3563.
Long, F., Zhu, A., Shi, H., Wang, H., 2014. Anal. Chem. 86, 2862–2866.
Marks, H.L., Pishko, M.V., Jackson, G.W., Cote, G.L., 2014. Anal. Chem. 86, 11614–11619.
Mei, Z., Chu, H., Chen, W., Xue, F., Liu, J., Xu, H., Zhang, R., Zheng, L., 2013a. Biosens. Bioelectron. 39, 26–30.
Mei, Z., Qu, W., Deng, Y., Chu, H., Cao, J., Xue, F., Zheng, L., El-Nezamic, H.S., Wu, Y., Chen, W., 2013b. Biosens. Bioelectron. 49, 457–461.
Paliwoda, R.E., Li, F., Reid, M.S., Lin, Y., Le, X.C., 2014. Anal. Chem. 86, 6138–6143.
Qian, L., Winfree, E., 2011. Science 332, 1196–1201.
Qian, L., Winfree, E., Bruck, J., 2011. Nature 475, 368–372.
Qing, Z., He, X., Huang, J., Wang, K., Zou, Z., Qing, T., Mao, Z., Shi, H., He, D., 2014. Anal. Chem. 86, 4934–4939.
Ragavan, K.V., Rastogi, N.K., Thakur, M.S., 2013a. Trends Anal. Chem. 52, 248–260.
Ragavan, K.V., Selvakumar, L.S., Thakur, M.S., 2013b. Chem. Commun. 49, 5960–5962.
Sadowski, J.P., Calvert, C.R., Zhang, D.Y., Pierce, N.A., Yin, P., 2014. ACS Nano 8, 3251–3259.
Sheng, Z., Zhu, B., 2011. Environ. Health Perspect. 119, 1775–1780.
Song, T., Xiao, S., Yao, D., Huang, F., Hu, M., Liang, H., 2014. Adv. Mater. 26, 6181–6185.
Tao, C., Yan, Y., Xiang, H., Zhu, D., Cheng, W., Ju, H., Ding, S., 2015. Chem. Commun. 51, 4220–4222.
Tharp, A.P., Maffini, M.V., Hunt, P.A., Vandevoort, C.A., Sonnenschein, C., Soto, A.M., 2012. Proc. Natl. Acad. Sci. USA 109, 8190–8195.
Vandenberg, L.N., Maffini, M.V., Sonnenschein, C., Rubin, B.S., Soto, A.M., 2009. Endocr. Rev. 30, 75–95.
Wang, F., Lu, C., Willner, I., 2014a. Chem. Rev. 114, 2881–2941.
Wang, K., Zhang, K., Lv, Z., Zhu, X., Zhu, L., Zhou, F., 2014b. Biosens. Bioelectron. 57, 91–95.
Wu, L., Wang, J., Ren, J., Qu, X., 2014. Adv. Funct. Mater. 24, 2727–2733.
Yin, P., Choi, H.M.T., Calvert, C.R., Pierce, N.A., 2008. Nature 451, 318–323.
You, M., Zhu, G., Chen, T., Donovan, M.J., Tan, W., 2015. J. Am. Chem. Soc. 137, 667–674.
Zhang, D.Y., Seelig, G., 2011. Nat. Chem. 3, 103–113.
Zhang, K., Ren, T., Wang, K., Zhu, X., Wu, H., Xie, M., 2014. Chem. Commun. 50, 13342–13345.
Zhang, L., Zhu, J., Zhou, Z., Guo, S., Li, J., Dong, S., Wang, E., 2013. Chem. Sci. 4, 4004–4010.
Zhu, Y., Cai, Y., Xu, L., Zheng, L., Wang, L., Qi, B., Xu, C., 2015. Appl. Mater. Interfaces 7, 7492–7496.